New Phytologist

Research

Gas exchange analysers exhibit large measurement error driven by internal thermal gradients

Josef C. Garen[1], Haley A. Branch[1], Isaac Borrego[1], Benjamin Blonder[2], Joseph R. Stinziano[3] and Sean T. Michaletz[1]

[1]Department of Botany and Biodiversity Research Centre, University of British Columbia, Vancouver, BC V6T 1Z4, Canada; [2]Department of Environmental Science, Policy, and Management, University of California, Berkeley, CA 94720, USA; [3]Canadian Food Inspection Agency, Ottawa, ON K1A 0Y9, Canada

Author for correspondence:
Josef C. Garen
Email: josef.garen@botany.ubc.ca

Received: *5 April 2022*
Accepted: *17 June 2022*

New Phytologist (2022) **236:** 369–384
doi: 10.1111/nph.18347

Key words: air temperature, ecophysiology, energy budget, leaf temperature, LI-6400XT, LI-6800, photosynthesis, thermoregulation.

Summary

- Portable gas exchange analysers provide critical data for understanding plant-atmosphere carbon and water fluxes, and for parameterising Earth system models that forecast climate change effects and feedbacks.
- We characterised temperature measurement errors in the Li-Cor LI-6400XT and LI-6800, and estimated downstream errors in derived quantities, including stomatal conductance (g_{sw}) and leaf intercellular CO_2 concentration (C_i).
- The LI-6400XT exhibited air temperature errors (differences between reported air temperature and air temperature measured near the leaf) up to 7.2°C, leaf temperature errors up to 5.3°C, and relative errors in g_{sw} and C_i that increased as temperatures departed from ambient. This caused errors in leaf-to-air temperature relationships, assimilation–temperature curves and CO_2 response curves. Temperature dependencies of maximum Rubisco carboxylation rate (V_{cmax}) and maximum RuBP regeneration rate (J_{max}) showed errors of 12% and 35%, respectively. These errors are likely to be idiosyncratic and may differ among machines and environmental conditions. The LI-6800 exhibited much smaller errors.
- Earth system model predictions may be erroneous, as much of their parametrisation data were measured on the LI-6400XT system, depending on the methods used. We make recommendations for minimising errors and correcting data in the LI-6400XT. We also recommend transitioning to the LI-6800 for future data collection.

Introduction

Plant physiology, ecophysiology and Earth system science have been greatly advanced by portable gas exchange analysers such as the Li-Cor LI-6400XT and LI-6800 (Li-Cor Biosciences, Lincoln, NE, USA). These instruments enable fine control of a leaf's environment and allow rapid, high-resolution measurements of leaf responses to varying conditions. Gas exchange measurements are widely used to develop and test theory, and to parameterise models for forecasting vegetation dynamics and climate change.

Gas exchange data play a crucial role in forecasting climate change and its effects on the biosphere. Process-based models, such as Earth system models (ESMs), simulate plant carbon uptake using the Farquhar–von Caemmerer–Berry (FvCB; Farquhar *et al.*, 1980) model of C_3 photosynthesis (Cramer *et al.*, 2001; Krinner *et al.*, 2005; Rogers *et al.*, 2017). The FvCB model requires parameters describing the maximum rate of Rubisco activity (V_{cmax}) and the maximum rate of RuBP regeneration (J_{max}), which are obtained from gas exchange measurements (Medlyn *et al.*, 2002; Kattge & Knorr, 2007; Galmés *et al.*, 2016). Similarly, ESMs estimate transpiration rates with models of stomatal conductance, such as the Ball–Berry-type models (Ball *et al.*, 1987; Leuning, 1995; Medlyn *et al.*, 2011), in which model parameters are also determined from gas exchange data (Medlyn *et al.*, 2011; Miner & Bauerle, 2017; Franks *et al.*, 2018). These parameters have a strong influence on predicted rates of photosynthesis, transpiration, and water-use efficiency (Jefferson *et al.*, 2017). In their sixth assessment report, the Intergovernmental Panel on Climate Change (IPCC) used a major ESM intercomparison project to inform projections of climate change effects on vegetation and feedbacks (Eyring *et al.*, 2016; IPCC, 2021). Therefore, our best predictions about climate change and its impacts are based directly on models parameterised with gas exchange data produced by these instruments.

Gas exchange analysers also play a pivotal role in the development and testing of plant ecophysiology theory. These instruments have been used to measure carbon assimilation rates central to the leaf economic spectrum (Wright *et al.*, 2004), and to test theory for leaf thermoregulation (Michaletz *et al.*, 2015, 2016; Blonder & Michaletz, 2018). Gas exchange measurements have also been used to test predictions for the allometric scaling of respiration (Reich *et al.*, 2006) and hypotheses for the activation energy of photosynthesis (Michaletz, 2018) in the metabolic theory of ecology (Brown *et al.*, 2004; Allen *et al.*, 2005). Given

the central role of gas exchange measurements in ESM predictions and physiological and ecological theory, accurate and reliable measurements are of paramount importance.

However, recent work has called into question the accuracy of leaf and air temperature measurements reported by these machines. C. J. Still *et al.* (2019) suggested that leaf-to-air temperature differences measured using the LI-6400XT may be misleading due to instrument design. They found that air within the cuvette will exhibit thermal gradients between the heat exchanger and the leaf temperature thermocouple, causing the appearance of leaf temperatures being offset toward ambient temperatures relative to reported cuvette air temperature (i.e. an apparent 'limited homeothermy' *sensu* Upchurch & Mahan, 1988), even without a leaf in the measurement cuvette. This leads to erroneous conclusions regarding leaf-to-air temperature relationships. Mott & Peak (2011) also reported biases in leaf temperatures measured by thermocouples in gas exchange cuvettes. They found that leaf temperatures measured by an uninsulated thermocouple in a gas exchange analyser were influenced by the temperature of the cuvette air across the leaf boundary layer and conduction along thermocouple wires, which led to measurement error when leaf and air temperatures differed. The authors further noted that temperature error may cause erroneous stomatal conductance readings. These studies suggest that temperature sensors in gas exchange analysers may not accurately report leaf and air temperatures, affecting conclusions relating to leaf physiology. In this paper, we build on these previous studies to directly measure the extent of these errors under different conditions and estimate their impact on derived quantities such as stomatal conductance and leaf intercellular CO_2 concentration.

As noted above, leaf temperature plays a critical role in the calculation of derived quantities reported by gas exchange analysers. The instruments directly measure leaf and air temperatures and concentrations of CO_2 and H_2O in air entering and leaving the cuvette, and use these as inputs for models that estimate quantities related to photosynthesis and transpiration (Li-Cor Biosciences Inc., 2012, 2019). For example, the LI-6400XT estimates leaf total conductance to water vapour g_{tw} (mol m^{-2} s^{-1}; please refer to Table 1) with the relationship

$$g_{tw} = \frac{E\left(1000 - \frac{W_l + W_s}{2}\right)}{W_l - W_s},$$

where E (mol m^{-2} s^{-1}) is the transpiration rate, W_s (mmol mol^{-1}) is the molar concentration of water vapour in the sample (air that has interacted with the leaf), and W_l (mmol mol^{-1}) is the molar concentration of water vapour in the leaf intercellular spaces. W_l is estimated using an exponential relationship between leaf temperature $T_{leaf,LI}$ and saturation vapour pressure, therefore measurement errors in $T_{leaf,LI}$ will lead to errors in g_{tw}. g_{tw} is then used to estimate stomatal conductance to water vapour g_{sw}, which is used to estimate leaf total conductance to CO_2 g_{tc}, and in turn g_{tc} is used to estimate leaf intercellular CO_2 concentration C_i. Errors in $T_{leaf,LI}$ may therefore propagate through these computations and into each of these derived quantities. In turn, all downstream analyses that depend on these reported quantities may also be affected.

Table 1 List of symbols.

Symbol	Description	Units
$T_{block,LI}$	Heat exchanger temperature; equivalent to T_{xchg} in LI-6800	°C
$T_{air,LI}$	Cuvette air temperature as reported by Li-Cor	°C
$T_{leaf,LI}$	Leaf temperature as reported by Li-Cor	°C
T_{amb}	Ambient air temperature surrounding Li-Cor	°C
$T_{air,lower}$	Air temperature in lower portion of cuvette measured by additional thermocouple	°C
$T_{air,upper}$	Air temperature in upper portion of cuvette measured by additional thermocouple	°C
$T_{leaf,lower}$	Leaf temperature on lower (abaxial) leaf surface measured by taped-on thermocouple	°C
$T_{leaf,thread}$	Internal leaf temperature measured by threaded thermocouple	°C
$T_{leaf,EB}$	Leaf temperature computed from energy balance	°C
g_{sw}	Stomatal conductance to water vapour	mol m^{-2} s^{-1}
g_{tw}	Leaf total conductance to water vapour	mol m^{-2} s^{-1}
g_{tc}	Leaf total conductance to CO_2	mol m^{-2} s^{-1}
C_i	Leaf intercellular CO_2 concentration	μmol mol^{-1}
T_{opt}	Optimal temperature for photosynthesis	°C
$T_{breadth}$	Thermal breadth of photosynthesis	°C
E_a	Activation energy of photosynthesis	eV
E_d	Deactivation energy of photosynthesis	eV
A_{max}	Peak photosynthetic rate	μmol m^{-2} s^{-1}

In this study, we examine how the thermal environments within the LI-6400XT and LI-6800 gas exchange analysers lead to error in measured temperatures and derived quantities, and how these errors affect downstream analysis. Our objectives are to: (1) characterise error in air and leaf temperatures due to the internal thermal environment of these instruments; (2) estimate error in derived quantities that depend on leaf temperature; and (3) use these error estimates to correct example data obtained from the LI-6400XT. We illustrate the extent of possible error in temperature and gas exchange measurements, and we provide recommendations for reducing or eliminating thermal bias and downstream errors when using gas exchange analysers. We also provide R code to back-correct LI-6400XT data files under certain conditions.

Materials and Methods

Overview of gas exchange analysers

The LI-6400XT and LI-6800 are shown schematically in Fig. 1. These instruments measure leaf-to-air carbon and water fluxes by calculating the difference in gas composition before and after exposure to leaf surfaces. The CO_2 and H_2O concentrations of incoming air are measured with an infrared gas analyser (IRGA) before the air is warmed or cooled by Peltier devices and delivered to the leaf cuvette. Air within the cuvette is exposed to the

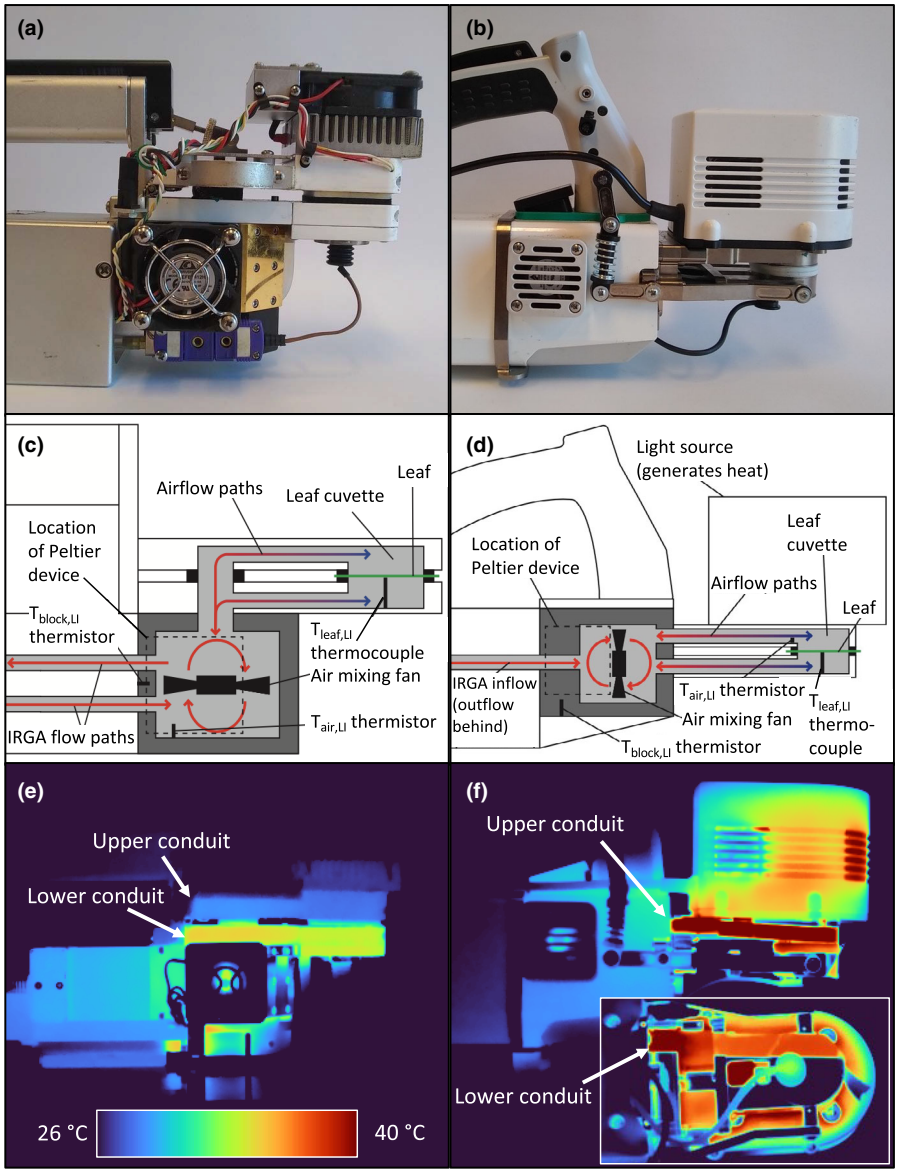

Fig. 1 Sensor heads of the LI-6400XT and LI-6800 gas exchange analysers, as illustrated by visual image (a, b), schematic diagram (c, d), and thermal image (e, f). (a, b) Side-view photographs of the LI-6400XT and LI-6800 sensor heads, respectively. (c, d) Diagrams showing key components of the airflow paths in the LI-6400XT and LI-6800, respectively, including the approximate location of air ($T_{air,LI}$), leaf ($T_{leaf,LI}$), and block ($T_{block,LI}$) temperature sensors, and illustrating air temperature gradients with high $T_{block,LI}$. (e, f) False colour thermal infrared images taken with a FLIR A700 thermal imaging camera of the LI-6400XT and LI-6800, respectively, with Peltier heating devices set to maximum $T_{block,LI}$. Inset in (f) shows the underside of LI-6800 with lower airflow conduit highlighted. Thermal gradients are apparent in the upper and lower airflow conduits in the LI-6400XT between the block and the cuvette; a substantial temperature difference is also apparent between the upper and lower air conduits. The lower conduit in the LI-6800 also shows a temperature gradient between the block and the cuvette.

surface of the leaf where gas exchange occurs. The air is circulated by a mixing fan throughout the cuvette and a second (sample) IRGA cell. The difference in CO_2 and H_2O concentrations in the air before and after exposure to the leaf are used to estimate variables of interest. Leaf and air temperatures are also measured, with air temperatures $T_{air,LI}$ being measured in substantially different locations along the air flow paths in the LI-6400XT and the LI-6800 (Fig. 1c,d).

Air and leaf temperatures

To investigate bias in air temperatures reported by the LI-6400XT and LI-6800, we conducted thermal performance trials in both instruments with no leaves in the cuvettes (Fig. 1). Airflow rate was 200 μmol s^{-1} with 10 000 rpm fan speed to promote cuvette air mixing (C. J. Still *et al.*, 2019). Ambient air temperature was 20°C. The lowest achievable heat exchanger temperature ($T_{block,LI}$) was selected and maintained until all temperature readings stabilised. $T_{block,LI}$, the reported cuvette air temperature measured by a thermistor ($T_{air,LI}$; Fig. 1), and $T_{leaf,LI}$ were recorded. $T_{block,LI}$ was increased in 4 or 5°C increments through the achievable temperature range of each machine (*c.* 0–50°C in the LI-6400XT and 6–44°C in the LI-6800), and the temperature readings were recorded at each step after stabilisation. To achieve extreme $T_{block,LI}$ values in the LI-6400XT, we used the 6400-88 Expanded Temperature Control Kit (Li-Cor Biosciences), which allows the operator to pass heated or cooled water through water jackets appressed to the Peltier devices. With no leaf in the cuvette, $T_{leaf,LI}$ measures the air temperature inside the cuvette; therefore we compared $T_{leaf,LI}$ to $T_{air,LI}$ to determine differences between the air temperatures reported by the machine and measured within the cuvette. Each trial was carried out on two replicate machines of each model (LI-6400XT manufacturing dates December 2008 and March 2014; LI-6800

manufacturing dates March 2018 and December 2019). Ordinary least squares (OLS) regression was performed on $T_{air,LI}$ vs $T_{leaf,LI}$.

We also conducted thermal performance trials between November 2019 and February 2022 using the broadleaf *Gaultheria shallon* Pursh (Ericaceae), and the scale-leaf *Thuja plicata* Donn ex D. Don (Cupressaceae). Plant material was collected at 95 m elevation at the University of British Columbia in Vancouver, Canada (49.26°N, 123.25°W). Intact branches were submerged in a pan of water and cut underwater to prevent embolism (Venturas *et al.*, 2015; Michaletz *et al.*, 2016; Wu *et al.*, 2020), then transported to the laboratory for immediate measurement. Cuttings maintained consistent gas exchange for more than 3 h, sufficient to complete our measurements. Leaves were placed into the cuvettes of the LI-6400XT and LI-6800 with additional insulated 32-gauge type K chromel-alumel thermocouples installed in the upper and lower portions of the cuvette to measure internal air temperatures ($T_{air,upper}$ and $T_{air,lower}$, respectively). These thermocouples were connected to either a TC-08 data acquisition board (Pico Technology, Cambridgeshire, UK) or a HH802W digital thermometer (Omega Engineering Inc., Norwalk, CT, USA). Putty (Loctite Fun-Tak or Hasbro Play-Doh) was used to seal air leaks in the cuvette gasket. Flow rate and fan speed were set as above, and photosynthetic photon flux density (PPFD) was set to 1600 μmol m^{-2} s^{-1}. Reference CO_2 concentration was maintained at 400 ppm. $T_{block,LI}$ was increased in 4 or 5°C increments, and temperature readings were allowed to stabilise at each increment. $T_{block,LI}$, $T_{air,LI}$, $T_{leaf,LI}$, $T_{air,upper}$ and $T_{air,lower}$ were recorded. This procedure was repeated with an empty cuvette as a control.

To investigate whether temperature biases in the LI-6400XT were driven by gradients between $T_{block,LI}$ and ambient air temperatures (T_{amb}), we eliminated these gradients by controlling T_{amb}. We repeated the procedure described in the previous paragraph with the LI-6400XT and LI-6800 placed inside an environmentally controlled growth chamber (PGR15; Conviron, Winnipeg, MB, Canada). While inside the growth chamber, the gas exchange analysers were stepped through their available temperature range in 4°C increments. At each temperature step, T_{amb} was set to match $T_{block,LI}$ at that step and the gas exchange analysers were allowed to equilibrate to their target temperatures for *c.* 20 min, and $T_{block,LI}$, $T_{air,LI}$, $T_{leaf,LI}$, $T_{air,upper}$ and $T_{air,lower}$ were recorded.

To investigate $T_{leaf,LI}$ measurement error, we measured abaxial leaf temperature $T_{leaf,lower}$ using insulated 36-gauge type-T copper-constantan thermocouples taped to the abaxial leaf surface using porous tape (3M Transpore). This method has been shown to accurately reproduce leaf temperature measured with infrared thermometry (Slot *et al.*, 2016). We taped 1 cm of thermocouple lead to the leaf to minimise heat transfer between the air and the thermocouple junction. We verified that the $T_{leaf,lower}$ accurately reported leaf internal temperatures by threading thermocouples 5 mm into secondary veins (Hanson & Sharkey, 2001) of a subset of the leaves, and found no significant difference (Supporting Information Fig. S1). Thermocouples measuring $T_{air,lower}$ and $T_{air,upper}$ were also installed as described above. Leaves with attached thermocouples were placed in the cuvettes, $T_{block,LI}$ was increased in 4 or 5°C increments, and $T_{block,LI}$, $T_{air,LI}$, $T_{leaf,LI}$, $T_{air,lower}$ and $T_{air,upper}$ were recorded. We also investigated the relationship of leaf temperature calculated by energy balance, $T_{leaf,EB}$, to $T_{leaf,lower}$. $T_{leaf,EB}$ was obtained by using the $T_{air,lower}$ reading as the air temperature value required by the calculation (normally supplied by $T_{leaf,LI}$), and recalculating $T_{leaf,EB}$ using the equations provided in the LI-6400XT operator's manual.

To visualise air temperature gradients within the machine, we obtained thermal images of the airflow conduits of each machine with a thermal imaging camera (A700; FLIR Systems Inc., Wilsonville, OR, USA). $T_{block,LI}$ was set to the maximum achievable value for each machine and readings were allowed to stabilise. High-emissivity (*c.* 0.95) black electrical tape was placed on the airflow conduits to improve accuracy. Thermal images were calibrated for distance, ambient temperature and relative humidity, with emissivity assumed to be 0.95, following Blonder *et al.* (2020).

Temperature readings from all thermocouples were checked against reference temperatures to ensure agreement (Fig. S2). Thermocouples were placed in a waterproof bag and submerged in a common water bath at temperatures spanning 5–45°C. The LI-6400XT and LI-6800 sensor heads were fixed above the water bath using tripods, allowing thermocouples to reach the water bath. $T_{block,LI}$ was maintained at 20°C. The LI-6800s had recent factory calibrations (within 2 yr) and LI-6400XT thermocouples were zeroed before measurement (Li-Cor Biosciences Inc., 2012). We noted a small bias in the LI-6400XT $T_{leaf,LI}$ readings relative to all other thermocouples (Fig. S2), which may be partly responsible for some of the errors discussed below. As these thermocouples were zeroed following Li-Cor specifications and the reported $T_{leaf,LI}$ is used in computation of derived quantities, we did not correct these readings.

Error in derived quantities

The quantities g_{tw}, g_{sw}, g_{tc} and C_i depend on $T_{leaf,LI}$, so measurement error in $T_{leaf,LI}$ may result in downstream errors in these derived quantities. Using estimates of error in $T_{leaf,LI}$ obtained in the previous section with the equations provided in the operator's manuals, we estimated error in g_{tw}, g_{sw}, g_{tc} and C_i.

We obtained raw LI-6400XT and LI-6800 output files for recalculating derived parameters. Data obtained from the LI-6400XT comprised 516 measurements of 73 leaves from 13 species of broadleaf herbs, shrubs, and graminoids native to the Rocky Mountains: *Artemisia tridentata*, *Balsamorhiza sagittate*, *Chamerion angustifolium*, *Dactylis glomerata*, *Delphinium barbeyi*, *Geranium viscosissimum*, *Ligusticum porteri*, *Lupinus argentenus*, *Pentaphylloides floribunda*, *Potentilla gracilis*, *Taraxacum officinale* *Valeriana occidentalis* and *Veratrum californicum*. The collection and measurement procedures for these data are described in Michaletz *et al.* (2016). For the LI-6800, we collected assimilation–temperature response (A–T) curves, with 459 measurements of 50 leaves from five species: *Borago officinalis*, *Hordeum vulgare*, *Raphanus sativus*, *Tilia tomentosa* and *Phaseolus vulgaris*. Data for both the LI-6400XT and LI-6800 were collated on the basis of

availability of raw output files. To balance sample sizes and ensure similar temperature distributions, we subsampled the datasets randomly within 5°C bins in $T_{leaf,LI}$, yielding 200 measurements for each Li-Cor model with roughly uniform distributions of $T_{leaf,LI}$ spanning 15–40°C.

Error in each of the values of g_{sw}, g_{tw}, g_{tc} and C_i was computed by estimating error in $T_{leaf,LI}$ for each measurement, subtracting error from $T_{leaf,LI}$, and recalculating the derived quantities using the corrected $T_{leaf,LI}$. Error in $T_{leaf,LI}$ was computed as ($T_{leaf,LI}$ − $T_{leaf,lower}$). A random slopes model using ($T_{air,LI}$ − $T_{leaf,LI}$) as a predictor was fitted to error in $T_{leaf,LI}$ with random effects for each measured leaf. This allowed us to account for substantial variability in slope and intercept observed between individual leaves. The predictor ($T_{air,LI}$ − $T_{leaf,LI}$) was chosen as it approximates the magnitude of leaf-to-air temperature difference (Mott & Peak, 2011), gives reasonable explanatory power, and is based on quantities reported by the machine (enabling postmeasurement correction for existing data sets without the need for additional thermocouples). Derived quantities were recalculated using equations provided in the operator's manuals (eqns 1-7 to 1-19, Li-Cor Biosciences Inc. (2012); eqns C-6 to C-16, Li-Cor Biosciences Inc. (2019)). Relative error δ was calculated as

$$\delta = \frac{m_{obs} - m_{corr}}{m_{corr}},$$

where m_{obs} and m_{corr} are the observed and corrected value of the quantity.

Correcting LI-6400XT datasets

To estimate error in relationships between leaf and air temperatures, we corrected $T_{air,LI}$ and $T_{leaf,LI}$ data from LI-6400XT machines. We measured $T_{air,LI}$ and $T_{leaf,LI}$ following Michaletz *et al.* (2016) for *Piper methysticum*, *Vicia faba*, *Coffea arabica*, *Carica papaya*, *Strelitzia reginae*, *Solanum melongena*, *Ricinus communus*, *Geraniaceae* sp., *Salacca magnifica*, and *Anthurium andraeanum* × *amnicola*. Measurements were taken from intact potted plants in the laboratory with ambient temperature at 20°C. All plants were mature individuals growing in the Department of Botany Teaching Greenhouse at the University of British Columbia. $T_{leaf,LI}$ was corrected as described in the previous section. $T_{air,LI}$ was corrected similarly, by fitting a random slopes model to error in $T_{air,LI}$ as a function of ($T_{air,LI}$ − $T_{block,LI}$), where error in $T_{air,LI}$ was taken as the difference between ($T_{air,upper}$ + $T_{air,lower}$)/2 and $T_{air,LI}$. (N.B. we refer to 'error in $T_{air,LI}$' throughout, because $T_{air,LI}$ misrepresents air temperature in the vicinity of the leaf. However, $T_{air,LI}$ may still accurately represent air temperature in the vicinity of the Peltier heaters.) The predictor was chosen as it reflects the magnitude and direction of the block-to-cuvette thermal gradients, gives reasonable explanatory power and is based on quantities directly reported by the machine. OLS regressions of corrected $T_{leaf,LI}$ vs corrected $T_{air,LI}$ were performed for each leaf to generate a frequency distribution of slopes.

To illustrate the effect of the temperature measurement errors on A–T curves, we measured an exemplary curve from *Anthurium andraeanum* × *amnicola*, following Michaletz *et al.* (2016). $T_{leaf,LI}$ values were corrected as described above. We estimated error in five parameters: optimal temperature for photosynthesis T_{opt}, activation energy E_a, deactivation energy E_d, maximum photosynthesis rate A_{max} and thermal breadth of photosynthesis $T_{breadth}$. We used the Sharp–Schoolfield model with high-temperature deactivation (Schoolfield *et al.*, 1981; Kontopoulos *et al.*, 2018) to estimate T_{opt}, E_a, and E_d, and a modified Gaussian model (Angilletta, 2006) to estimate A_{max} and $T_{breadth}$. Models were fitted using nonlinear least squares (NLS) regression and the NLS.MULTSTART and RTPC packages (Padfield *et al.*, 2021).

To estimate the effect of temperature measurement errors on A–C_i curves, we used the LI-6400XT to measure A–C_i curves in leaves of *Phaseolus vulgaris*. A–C_i curves were measured at $T_{block,LI}$ = 14, 20, 26, 32, and 38°C. Reference CO_2 spanned 50 to 1800 ppm, and PPFD was maintained at 800 μmol m^{-2} s. $T_{leaf,LI}$ and C_i were corrected as described above. V_{cmax} and J_{max} were estimated by fitting the FvCB model to each curve using the PLANTECOPHYS package (Duursma, 2015). We estimated E_a and the V_{cmax} or J_{max} value at 25°C, k_{25}, by fitting an Arrhenius function (Medlyn *et al.*, 2002) to the corrected and uncorrected V_{cmax} and J_{max} data as a function of corrected and uncorrected $T_{leaf,LI}$ using NLS regression.

All analyses were performed in R v.3.6.2 (R Core Team, 2019), using GGPLOT2 (Wickham, 2009), GRIDEXTRA (Auguie, 2017), and TIDYVERSE (Wickham *et al.*, 2019).

Results

Air and leaf temperatures

With an empty cuvette, relationships between measured and reported cuvette air temperatures varied between the LI-6400XT and the LI-6800 (Fig. 2). In the LI-6400XT, air temperature measured by $T_{leaf,LI}$ varied with reported air temperature $T_{air,LI}$ with a slope of 0.69 (95% confidence interval (95% CI) = 0.67 to 0.71; r^2 = 1.00) and an intercept of 7.39°C (95% CI = 7.10 to 7.69). $T_{leaf,LI}$ is elevated relative to $T_{air,LI}$ at low $T_{air,LI}$ and depressed relative to $T_{air,LI}$ at high $T_{air,LI}$, showing a departure from $T_{air,LI}$ by as much as 8°C at temperature extremes (Fig. 2b). By contrast, the LI-6800 shows a relationship between $T_{leaf,LI}$ and $T_{air,LI}$ with a slope of 0.99 that is not significantly different from 1 (95% CI = 0.97 to 1.02; r^2 = 1.00), but an intercept of 0.90°C that is significantly greater than 0 (95% CI = 0.20 to 1.59), indicating that cuvette air temperatures were generally higher than reported by the instrument (Fig. 2b).

Placement of additional thermocouples measuring $T_{air,lower}$ and $T_{air,upper}$ revealed that the agreement between measured and reported air temperatures varied between lower and upper portions of the cuvette (Fig. 3a,c). In the LI-6400XT, $T_{air,upper}$ exhibited a slope of 0.61 relative to $T_{air,LI}$ (95% CI = 0.59 to 0.63; r^2 = 0.98) with an intercept of 10.1°C (95% CI = 9.5 to 10.7), whereas $T_{air,lower}$ showed a slope of 0.85 (95% CI = 0.85 to 0.86; r^2 = 1.00) with an intercept of 3.9°C (95% CI = 3.7 to 4.0), indicating that $T_{air,upper}$ and $T_{air,lower}$ were closer to T_{amb} than $T_{air,LI}$. For a given $T_{air,LI}$, $T_{air,upper}$ was closer to T_{amb} than

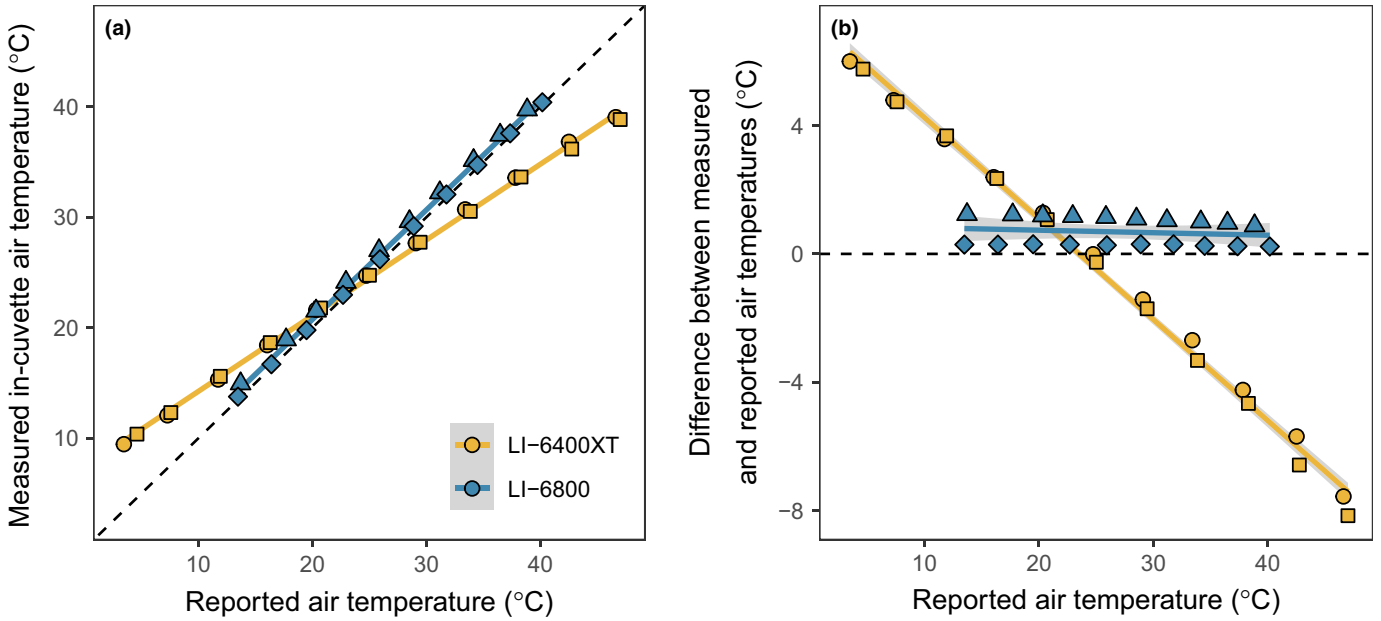

Fig. 2 Relationships between reported air temperature ($T_{air,LI}$) and measured in-cuvette air temperature (measured by leaf thermocouple, $T_{leaf,LI}$) in the LI-6400XT and LI-6800 without leaves in the cuvettes. (a) Measured in-cuvette air temperature ($T_{leaf,LI}$) as a function of reported air temperature ($T_{air,LI}$). Dashed line is 1 : 1. (b) Difference between measured in-cuvette air temperature and reported air temperature ($T_{leaf,LI} - T_{air,LI}$) as a function of reported air temperature ($T_{air,LI}$). Dashed line at zero indicates no difference between measured and reported air temperatures at a given $T_{air,LI}$. Different symbol shapes indicate different machines of the same model. With an empty cuvette, reported leaf temperature $T_{leaf,LI}$ measures in-cuvette air temperature.

$T_{air,lower}$, resulting in an air temperature gradient from the upper to lower portion of the cuvette that grew in magnitude toward temperature extremes (Fig. 3c). With no leaf in the cuvette, differences between $T_{air,lower}$ and $T_{air,upper}$ were diminished but not eliminated (Fig. 3a,c). Thermocouples were swapped between upper and lower cuvette portions to ensure this was not a calibration effect.

We found much closer agreement between measured and reported air temperatures in the LI-6800 (Fig. 3b,d). The slope of $T_{air,upper}$ with respect to $T_{air,LI}$ was not distinguishable from 1 (slope = 0.99, 95% CI = 0.98 to 1.00, r^2 = 1.00; intercept = 0.68°C, 95% CI = 0.37 to 1.0), and the slope of $T_{air,lower}$ with respect to $T_{air,LI}$ was only marginally different from 1 (slope = 0.97, 95% CI = 0.96 to 0.98, r^2 = 1.00; intercept = 0.08°C, 95% CI = −0.31 to 0.46), indicating strong agreement. The in-cuvette air temperature gradients were also reduced in magnitude, and both $T_{air,upper}$ and $T_{air,lower}$ departed from $T_{air,LI}$ by no more than 2.1°C (Fig. 3d). $T_{air,upper}$ was on average 1.1°C greater than $T_{air,lower}$ (Fig. 3d), resulting in an air temperature gradient within the cuvette of a substantially smaller magnitude than in the LI-6400XT (Fig. 3c). The observed relationships are similar with no leaf in the chamber, although the difference between $T_{air,upper}$ and $T_{air,lower}$ is reduced to 0.5°C.

Using a growth chamber for ambient temperature control eliminated differences between T_{amb} and $T_{block,LI}$, and eliminating $T_{air,LI}$ bias toward ambient (Figs 1, 4). When T_{amb} = $T_{block,LI}$, $T_{air,upper}$ and $T_{air,lower}$ in the LI-6400XT increased with $T_{air,LI}$ with slopes indistinguishable from 1, indicating no $T_{air,LI}$ bias toward ambient (Fig. 4a,c; $T_{air,upper}$ slope = 0.99, 95% CI = 0.98 to 1.00, r^2 = 1.00; $T_{air,lower}$ slope = 0.99, 95% CI = 0.97 to 1.00, r^2 = 1.00). The intercept was significantly greater than 0 for both $T_{air,upper}$ (2.0°C, 95% CI = 1.7 to 2.2) and $T_{air,lower}$ (1.0°C, 95% CI = 0.58 to 1.4), indicating that measured air temperatures exceeded reported air temperatures. The LI-6800 also showed no $T_{air,LI}$ bias toward ambient when the ambient-to-block temperature differences were eliminated (Fig. 4b,d). $T_{air,upper}$ and $T_{air,lower}$ varied with $T_{air,LI}$ in the LI-6800 with slopes not statistically different from 1 ($T_{air,upper}$ slope = 1.01, 95% CI = 0.99 to 1.02, r^2 = 1.00; $T_{air,lower}$ slope = 1.02, 95% CI = 0.99 to 1.04, r^2 = 1.00). Furthermore, the relationship between $T_{air,upper}$ and $T_{air,LI}$ had an intercept not distinct from 0 (0.19°C, 95% CI = −0.14 to 0.53), indicating that in the LI-6800, $T_{air,LI}$ accurately reported upper-cuvette air temperatures. However, the intercept between $T_{air,lower}$ and $T_{air,LI}$ was significantly less than zero (−1.4°C, 95% CI = −2.2 to −0.69).

Thermal imaging revealed temperature gradients along the airflow paths in both the LI-6400XT and the LI-6800 (Fig. 1e,f). With $T_{block,LI}$ set to the maximum value achievable without external temperature control (39.8°C in the LI-6400XT and 51.1°C in the LI-6800), the LI-6400XT shows differences between the upper and lower airflow conduits, with the upper conduit being noticeably closer to ambient temperature than the lower conduit. Both airflow paths show slight thermal gradients between the block and the cuvette, with the upper conduit decreasing from 28.6 to 27.9°C and the lower conduit from 34.6 to 33.6°C. There were also noticeable differences between airflow paths in the LI-6800. At 41°C, the upper conduit was warmer than the lower conduit, but only the lower conduit showed evidence of a block-to-cuvette gradient, decreasing from 41.2 to 37.8°C. These results are consistent with the patterns of in-cuvette air temperatures noted previously.

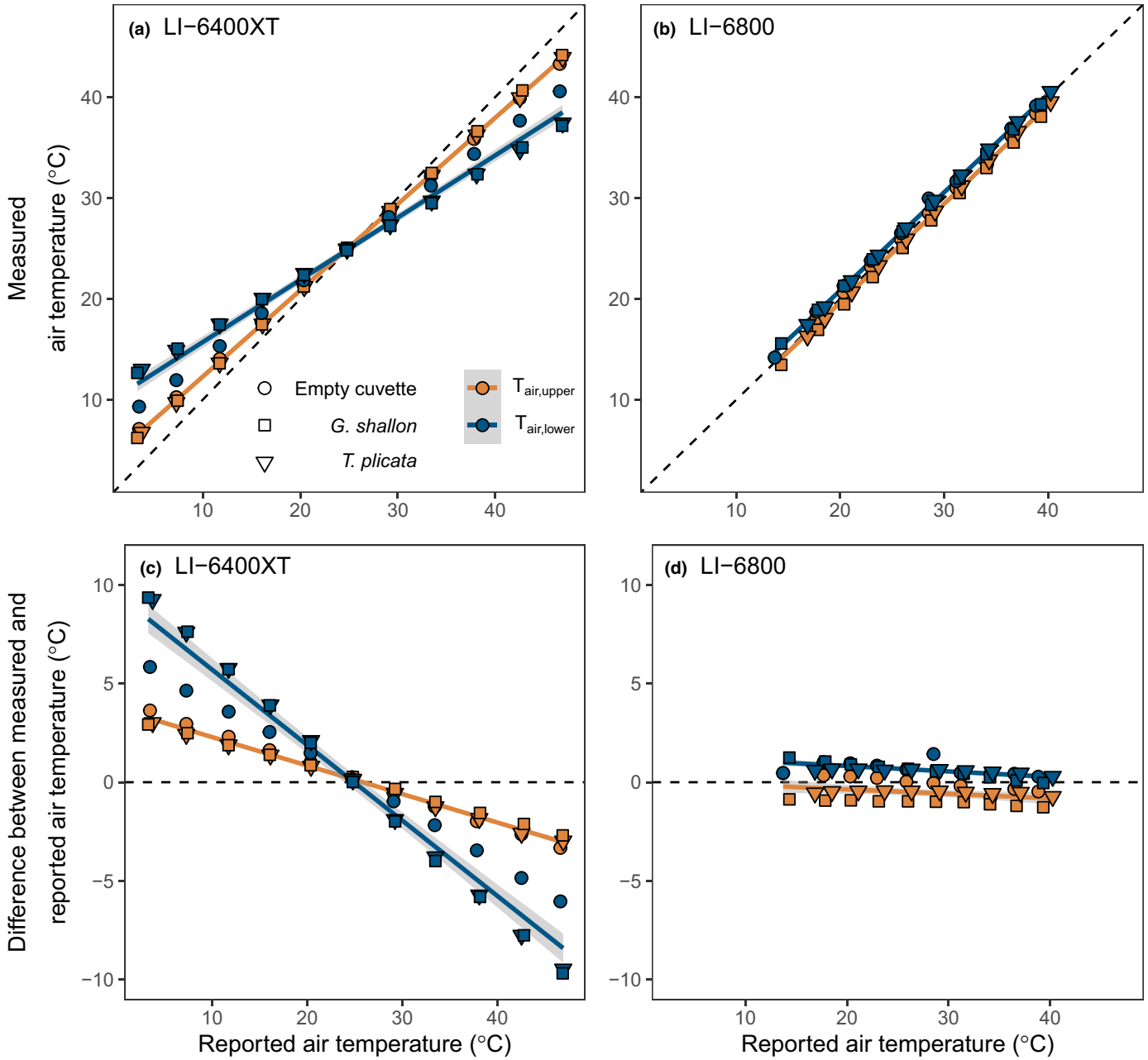

Fig. 3 Relationships between measured air temperatures above or below the plane of the leaf and instrument-reported air temperatures. Measured in-cuvette air temperatures ($T_{air,upper}$ and $T_{air,lower}$) are shown as functions of air temperature reported by the machines ($T_{air,LI}$) in (a) the LI-6400XT and (b) the LI-6800. The difference between air temperatures in the cuvette as measured by additional thermocouples above or below the plane of the leaf and reported air temperature ($T_{air,upper} - T_{air,LI}$ and $T_{air,lower} - T_{air,LI}$) are shown as functions of reported air temperature ($T_{air,LI}$) in (c) the LI-6400XT and (d) the LI-6800. Trials are shown using leaves of *Gaultheria shallon*, *Thuja plicata* and an empty cuvette. Blue symbols indicate cuvette air temperatures measured below the plane of the leaf ($T_{air,lower}$), and orange symbols indicate cuvette air temperatures measured above the plane of the leaf ($T_{air,upper}$).

Both machines showed errors in $T_{leaf,LI}$, with a larger range of error values in the LI-6400XT than the LI-6800 (Fig. 5). Fig. 5a shows error in $T_{leaf,LI}$ as a function of ($T_{air,LI} - T_{leaf,LI}$). $T_{leaf,LI}$ error in the LI-6400XT exhibited substantial variability. The mean slope determined from our mixed effects model was 0.53 with respect to ($T_{air,LI} - T_{leaf,LI}$) (95% CI = 0.26 to 0.80) and an intercept of −0.88°C (95% CI = −1.51 to −0.24). $T_{leaf,LI}$ error in the LI-6800 exhibited a slope of 0.45 with respect to ($T_{air,LI} - T_{leaf,LI}$) (95% CI = 0.37 to 0.53) with an intercept of −1.0°C (95% CI = −1.2 to −1.0). In the LI-6800, $T_{leaf,LI}$ consistently underestimated the leaf internal temperature by an average of 0.9°C. However, ($T_{air,LI} - T_{leaf,LI}$) values were overall much lower in magnitude in the LI-6800, resulting in a smaller range of $T_{leaf,LI}$ error. In the LI-6400XT, ($T_{air,LI} - T_{leaf,LI}$) ranged from −6.7 to +5.4°C, resulting in a range of $T_{leaf,LI}$ error from −5.3 to +1.2°C. In

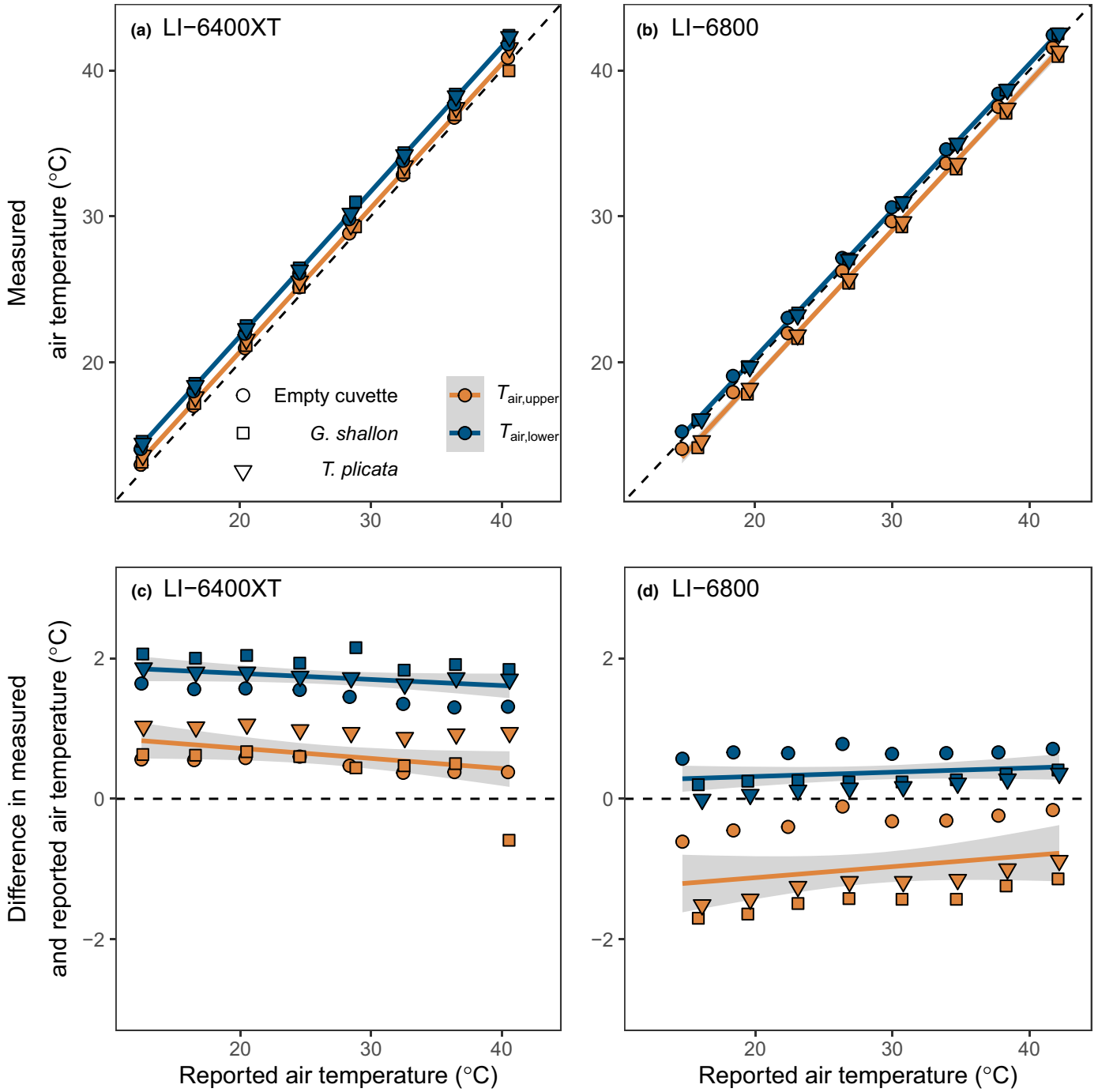

Fig. 4 Relationships between air temperatures measured above and below the plane of the leaf and instrument-reported air temperatures, with external ambient air temperature control. Measured in-cuvette air temperatures ($T_{air,upper}$ and $T_{air,lower}$) are shown as functions of air temperature reported by the machines ($T_{air,LI}$) in (a) the LI-6400XT and (b) the LI-6800. Differences between air temperature in the cuvette as measured by additional thermocouples above and below the plane of the leaf and reported air temperature ($T_{air,upper} - T_{air,LI}$ and $T_{air,lower} - T_{air,LI}$, respectively) are shown as functions of reported air temperature ($T_{air,LI}$) in (c) the LI-6400XT and (d) the LI-6800. Trials are shown using leaves of *Gaultheria shallon*, *Thuja plicata* and an empty cuvette. Blue symbols indicate cuvette air temperatures measured below the plane of the leaf ($T_{air,lower}$), and orange symbols indicate cuvette air temperatures measured above the plane of the leaf ($T_{air,upper}$). Li-Cor machines were placed in a environmentally controlled plant growth chamber, and the ambient air temperature in the growth chamber (T_{amb}) was matched to the heat exchanger temperature ($T_{block,LI}$) at each measurement temperature.

the LI-6800, ($T_{air,LI} - T_{leaf,LI}$) ranged from −0.58 to +1.4°C, resulting in a range of $T_{leaf,LI}$ error from −1.5 to −0.16°C. In the LI-6400XT, $T_{leaf,EB}$ also showed errors that depended on temperature (Fig. S3). $T_{leaf,EB}$ overestimated $T_{leaf,lower}$ at high temperatures and underestimated $T_{leaf,lower}$ at low temperatures, exhibiting a slope of 1.36 (95% CI = 1.34 to 1.39, r^2

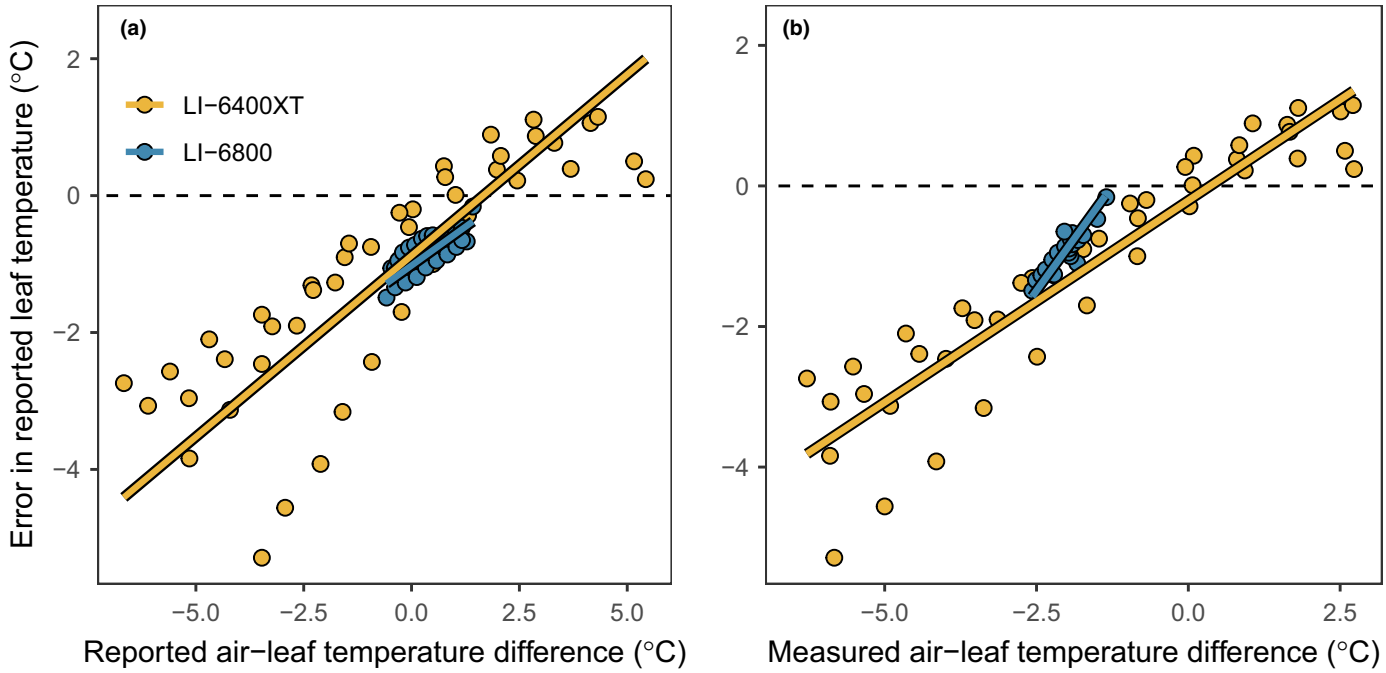

Fig. 5 Error in leaf temperatures reported by the internal leaf thermocouples in the LI-6400XT and LI-6800. (a) Error in $T_{leaf,LI}$ (measured as $T_{leaf,LI} - T_{leaf,lower}$) as a function of machine-reported difference in air and leaf temperatures ($T_{air,LI} - T_{leaf,LI}$). (b) Error in $T_{leaf,LI}$ (measured as $T_{leaf,LI} - T_{leaf,lower}$) as a function of measured difference in air and leaf temperatures ($T_{air,lower} - T_{leaf,lower}$). Lines show fixed effects of best fit random slopes models.

= 1.00) and intercept of −8.4°C (95% CI = −9.1 to −7.6). At the high-temperature extreme, $T_{leaf,EB}$ overestimated $T_{leaf,lower}$ by 6.7°C, and at the low temperature extreme, $T_{leaf,EB}$ underestimated $T_{leaf,lower}$ by 4.0°C.

Comparing error in reported $T_{leaf,LI}$ to ($T_{air,lower} - T_{leaf,lower}$) revealed different dependencies of $T_{leaf,LI}$ error on air-to-leaf temperature differences (Fig. 5b). In the LI-6400XT, $T_{leaf,LI}$ exhibited error with a slope of 0.57 with respect to $T_{air,lower} - T_{leaf,lower}$ (95% CI = 0.40 to 0.75; intercept = −0.21°C, 95% CI = −0.45 to 0.04), whereas the LI-6800 showed a slope of 1.19 (95% CI = 1.00 to 1.38; intercept = 1.49°C, 95% CI = 1.02 to 1.96).

Error in derived quantities

The range of error for all derived quantities was substantially greater in the LI-6400XT than the LI-6800 (Fig. 6). In both the LI-6400XT and the LI-6800, the distribution of errors centred close to zero, with median absolute relative errors < 2% for both machines in all derived quantities. The spread of errors was substantially greater in the LI-6400XT, however, with standard deviations of 19%, 18%, 18%, and 16% in g_{sw}, g_{tw}, g_{tc} and C_i, respectively, compared with 9%, 8%, 8%, and 5% in the LI-6800 (Fig. 6a). The error observed in derived quantities depended on machine conditions, and could be extremely large, especially in the LI-6400XT (Fig. 6b–e). The error magnitude in derived quantities depends on error in $T_{leaf,LI}$, which is well predicted by $T_{leaf,LI} - T_{air,LI}$ (Fig. 5a). Therefore when $T_{leaf,LI}$ and $T_{air,LI}$ are similar, errors in $T_{leaf,LI}$ and derived quantities are small, whereas when $T_{leaf,LI}$ departs substantially from $T_{air,LI}$, these errors are large.

Correcting LI-6400XT datasets

The regression results of Table 2 were used to correct LI-6400XT datasets for the errors described above. We provide an R script to correct LI-6400XT files at https://github.com/MichaletzLab/LI-COR-thermal-gradients.

We corrected errors in $T_{leaf,LI}$ and $T_{air,LI}$ measurements (Fig. 7), resulting in altered slopes in the relationship between in $T_{leaf,LI}$ and $T_{air,LI}$. Corrected data exhibited a higher mean slope than uncorrected data, with an uncorrected mean slope of 0.70 (95% CI = 0.68 to 0.71) and a corrected mean slope of 0.79 (95% CI = 0.75 to 0.83). Corrected slopes display a broader range of values than uncorrected slopes (Fig. 7 insets), but all slopes were < 1 (exhibiting limited homeothermy).

We corrected leaf temperature errors in an A–T curve, which strongly altered the relationship (Fig. 8). Estimates of key parameters are summarised in Table 3. Correction shifted leaf temperatures towards ambient, which significantly increased T_{opt} from 20.7 to 24.3°C ($F = 18.7$, $P = 0.0007$), decreased $T_{breadth}$ from 13.8 to 10.6°C ($F = 14.6$, $P = 0.001$), and increased the deactivation energy E_d from 1.36 to 1.73 eV ($F = 5.99$, $P = 0.03$). Correction also substantially increased the estimate of E_a from 0.96 to 1.15 eV, although this was not statistically significant ($F = 0.85$, $P = 0.37$), while A_{max} remained unchanged at 3.4 μmol m^{-2} s^{-1} ($F = 0.077$, $P = 0.78$).

We corrected A–C_i curves, resulting in dramatic differences in estimates of V_{cmax}, J_{max}, and corresponding temperature response parameters (Fig. 9). Corrected V_{cmax} and J_{max} values were shifted in a manner that depended on temperature. At lower temperatures, V_{cmax} increased and J_{max} decreased after correction, whereas at higher temperatures V_{cmax} decreased and J_{max} increased. These

New Phytologist

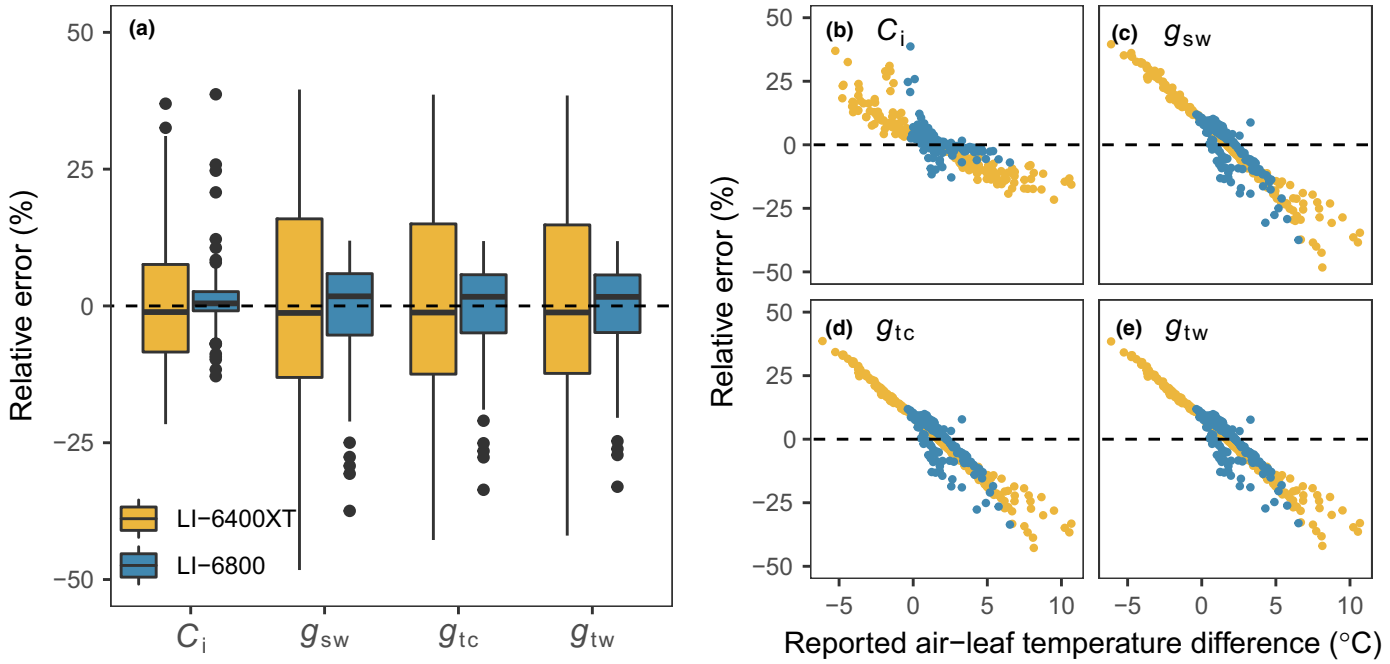

Fig. 6 Error in reported leaf temperatures drives error in derived quantities reported by the LI-6400XT and LI-6800. $T_{leaf,LI}$ error estimates are based on the regressions given in Table 2, and derived quantities g_{sw} (leaf stomatal conductance to water), g_{tw} (leaf total conductance to water), g_{tc} (leaf total conductance to CO_2), and C_i (leaf intercellular CO_2 concentration) were recalculated using corrected $T_{leaf,LI}$ values. (a) Distributions of errors by variable and type of Li-Cor machine. Smaller panels show the dependence of (b) g_{sw}, (c) g_{tw}, (d) g_{tc}, and (e) C_i on ($T_{air,LI} - T_{leaf,LI}$) for each type of Li-Cor machine. These estimates provide a representative distribution of errors across the temperature range achievable by both machines without external temperature control (15–40°C in reported $T_{leaf,LI}$).

Table 2 Parameter values ± SE for linear regressions estimating error in leaf and air temperatures in the LI-6400XT.

Response (°C)	Predictor (°C)	Slope (dimensionless)	Intercept (°C)	*P*
Error in $T_{air,LI}$	$T_{block,LI} - T_{air,LI}$	2.2835 ± 0.1043	−0.3456 ± 0.0834	$< 10^{-5}$
Error in $T_{leaf,LI}$	$T_{air,LI} - T_{leaf,LI}$	0.5296 ± 0.1328	−0.8771 ± 0.3129	0.0003

$T_{air,LI}$, cuvette air temperature as reported by Li-Cor; $T_{block,LI}$, heat exchanger temperature; $T_{leaf,LI}$, leaf temperature as reported by Li-Cor.

shifts were reflected in the Arrhenius model parameters fit to each dataset. For V_{cmax}, E_a decreased from 68.8 to 61.2 kJ mol^{-1} K^{-1} (marginally significant; $F = 4.48$, $P = 0.08$). k_{25} of V_{cmax} was essentially unchanged, moving from 74.9 to 74.1 µmol m^{-2} s^{-1} ($F = 0.20$, $P = 0.67$). For J_{max}, E_a increased significantly from 28.5 to 36.2 kJ mol^{-1} K^{-1} ($F = 8.31$, $P = 0.028$). k_{25} of J_{max} decreased slightly, but not significantly, from 119.5 to 116.4 µmol m^{-2} s^{-1} ($F = 2.9$, $P = 0.14$).

Discussion

In this paper, we (1) characterised error in measurements of air and leaf temperatures in the LI-6400XT and LI-6800 gas exchange analysers; (2) estimated error in derived quantities that depend on measured leaf temperature; and (3) used these error estimates to correct example data obtained from the LI-6400XT. For (1), we observed that measured air temperature in the LI-6400XT was substantially biased toward ambient air temperature (Figs 2, 3), and that internal air temperature gradients drove large errors in $T_{leaf,LI}$ and $T_{air,LI}$ (Figs 3, 4). For (2), we demonstrated large errors in g_{tw}, g_{sw}, g_{tc} and C_i when $T_{block,LI}$ departed from T_{amb} in the LI-6400XT (Fig. 6). In the LI-6800, these errors were greatly reduced (Figs 2–6). For (3), we used our error estimates to correct example LI-6400XT datasets, showing that these errors strongly influenced the relationships between air temperature and leaf temperature (Fig. 7), net photosynthesis (Fig. 8), and A–C_i curves (Fig. 9). Correction of these relationships revealed errors in estimates of T_{opt}, $T_{breadth}$, V_{cmax}, J_{max} and other key parameters.

Thermal gradients drive leaf and air temperature errors

In the LI-6400XT, when $T_{block,LI}$ departed from T_{amb}, large errors in $T_{air,LI}$ and $T_{leaf,LI}$ were found. $T_{air,LI}$ errors appear to be driven by heat transfer between the air and airflow conduits as the air travels to the cuvette (C. J. Still *et al.*, 2019). Because the $T_{air,LI}$ thermistor is located near the Peltier device (Fig. 1), this thermal gradient means that $T_{air,LI}$ does not reflect in-cuvette conditions. Reported leaf-to-air temperature relationships therefore appear to display limited homeothermy, even if this

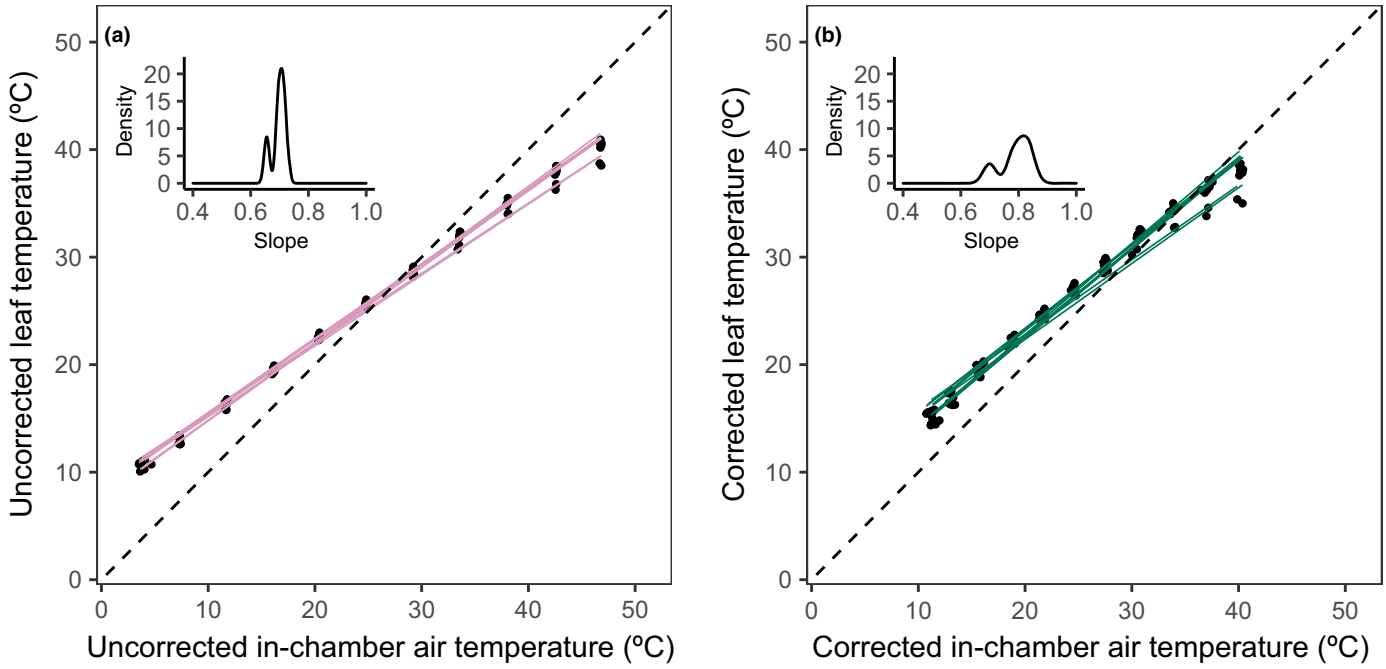

Fig. 7 Limited homeothermy in 10 leaves from different species of broadleaf plants. Relationships between leaf temperature and cuvette air temperature are shown (a) before and (b) after correction of temperature measurement error. Dashed lines are a 1 : 1 relationship. Insets show frequency distributions of fitted slopes. In panel (b), data were corrected using regression coefficients from Table 2.

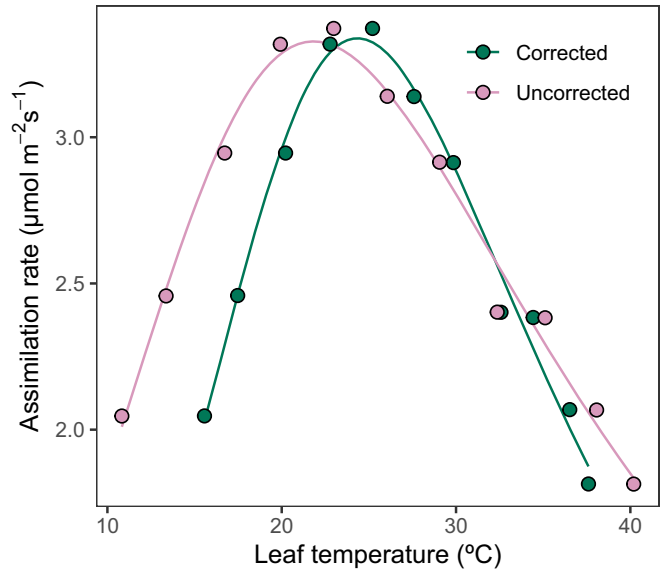

Fig. 8 Assimilation–temperature response curves for *Anthurium andraeanum* × *amnicola* leaves measured with an LI-6400XT, before and after correction of temperature measurement error. Leaf temperature data were corrected using the regression coefficients in Table 2. Lines represent model predictions from the best fit Sharpe–Schoolfield temperature response function with high-temperature deactivation. Best fit parameters are given in Table 3.

behaviour is not occurring (N.B. limited homeothermy may still occur in the leaf cuvette; Fig. 7b). These internal air temperature gradients are reflected in the surface temperatures of the air conduits observed via thermal imaging (Fig. 1). While thermal gradients occur in the LI-6800 as well (Fig. 1f, inset), the air temperature thermistor is located immediately adjacent to the cuvette and therefore better reflects in-chamber air temperature, resulting in much smaller errors in $T_{air,LI}$.

In the LI-6400XT, error in $T_{leaf,LI}$ appears to be driven by differences in air and leaf temperatures (Mott & Peak, 2011). The LI-6400XT leaf thermocouple is uninsulated, so the junction and lead wires are exposed to convective heat transfer from circulating air during measurement. The energy balance of the leaf is determined in part by the temperature of air in the immediate vicinity of the leaf and the leaf boundary layer (which is relatively thin in the cuvette environment). This further demonstrates the importance of measuring air temperature as near to the leaf surface as possible. These issues appear to be largely resolved in the LI-6800 due to improved design of the leaf thermocouple. Our results suggest that the LI-6400XT should not be used for measurements in which substantial temperature control is desired unless ambient temperature around the instrument is also controlled.

Energy balance is widely used as an alternative method for estimating leaf temperature, especially when thermocouple contact with the leaf is poor (e.g. needle leaves), or to compensate for temperature biases (C. J. Still *et al.*, 2019). However, our results suggest that $T_{leaf,EB}$ exhibits similar thermal biases when the LI-6400XT is controlled to depart from ambient temperature. $T_{leaf,EB}$ approximates measured leaf temperature when machine conditions are near ambient, but $T_{leaf,EB}$ under- or over-estimates leaf temperature at low and high temperatures, respectively (Fig. S3). This is likely because $T_{air,LI}$ serves as an approximation for cuvette wall temperature in the

New Phytologist

Table 3 Parameter estimates for models fitted to the uncorrected and corrected assimilation–temperature response curves for *Anthurium andraeanum* × *amnicola* in Fig. 8.

Parameter	Units	Uncorrected estimate	Corrected estimate	*P*	Fitted model
T_{opt}	°C	21.8	24.3	0.00071	Sharpe–Schoolfield
E_a	eV	0.96	1.15	0.37	Sharpe–Schoolfield
E_d	eV	1.36	1.73	0.028	Sharpe–Schoolfield
A_{max}	μmol m^{-2} s^{-1}	3.43	3.41	0.78	Modified Gaussian
$T_{breadth}$	°C	13.9	10.6	0.0015	Modified Gaussian

A_{max}, peak photosynthetic rate; E_a, activation energy of photosynthesis; E_d, deactivation energy of photosynthesis; $T_{breadth}$, thermal breadth of photosynthesis; T_{opt}, optimal temperature for photosynthesis.

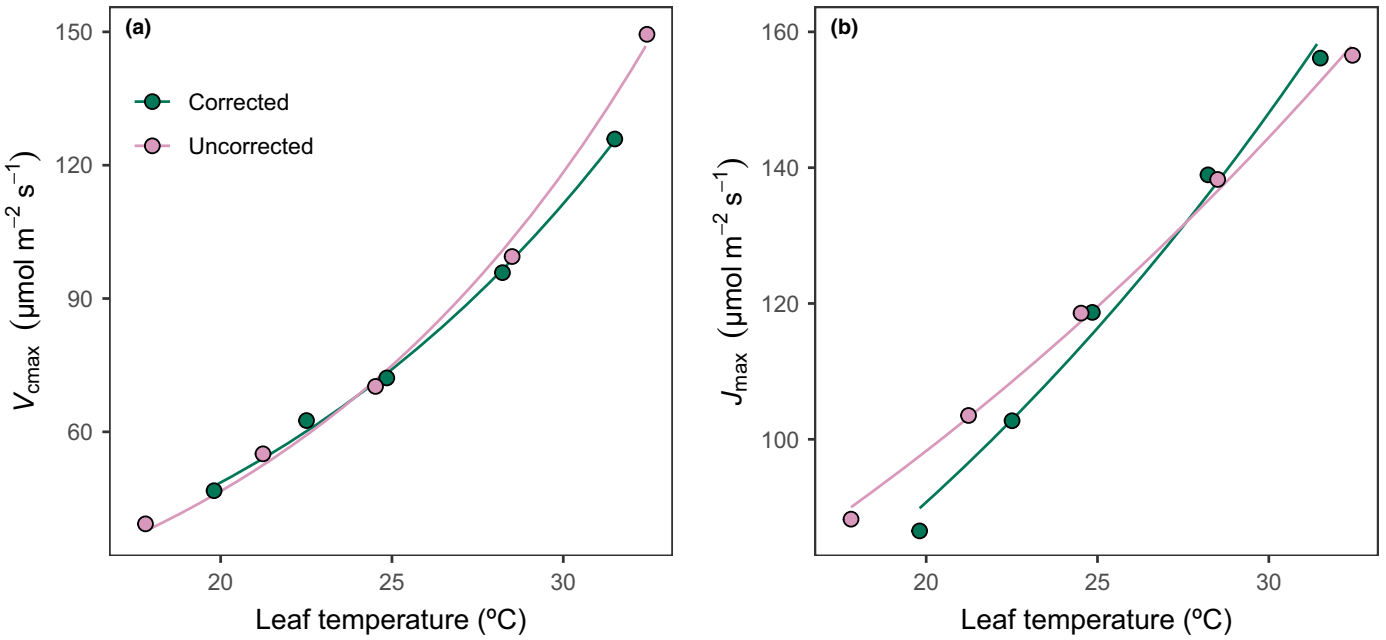

Fig. 9 Temperature response of (a) maximum rate of Rubisco carboxylation (V_{cmax}) and (b) maximum rate of RuBP regeneration (J_{max}) measured in leaves of *Phaseolus vulgaris* with the LI-6400XT before and after correction for leaf temperature error. Leaf temperatures were corrected using regression coefficients in Table 2, and corrected leaf temperatures were used to correct C_i (intercellular CO_2 concentration) values according to the equations presented in the LI-6400XT manual before estimating V_{cmax} and J_{max}. Lines represent best fit Arrhenius temperature response functions.

LI-6400XT energy balance calculation, and this approximation becomes less accurate as the block reaches high or low temperatures (p. 17-8; Li-Cor Biosciences Inc., 2012). Therefore, when temperature control outside of ambient conditions is desired, the energy balance calculation fails to avoid the issues described here. We suggest that operators follow similar suggestions to reduce error, such as taking measurements at ambient conditions or controlling ambient temperature, even if using $T_{leaf,EB}$.

Ultimately, the thermal behaviour of these machines is determined by the energy balance of the sensor heads, which is influenced by the internal and external environments (c.f. Gates, 1980; Bergman *et al.*, 2011; Monteith & Unsworth, 2013). Their behaviour is affected by the temperature of incoming air, ambient temperature, incident radiation, heating or cooling by the Peltier devices, and other variables. Because of this, the error estimates and corrections developed here may not apply universally. Our results should be therefore interpreted as exemplary of the extent of errors possible when using gas exchange equipment. The postmeasurement correction code was parameterised using data collected in laboratory conditions (low light, 20°C ambient temperature). Operators of gas exchange instruments are urged to test for these error effects in their own machines and environmental conditions, and to parameterise the correction functions for their own conditions before applying our postmeasurement correction code. The corrections are likely to be different when environmental conditions differ (high or low ambient temperatures, high incident light). Furthermore, if ambient conditions are highly variable, reliably postcorrecting data in this manner may not be possible.

Although we were not able to test this here, other gas exchange systems (e.g. Walz GFS-3000, PP Systems CIRAS-3) may also exhibit thermal biases, and we suggest users of those machines test for these effects as well.

Effects of temperature error on limited homeothermy

Correcting leaf and air temperature relationships resulted in a substantially altered distribution of slopes of leaf temperature relative to air temperature, but all measured leaves still exhibited limited homeothermy. Leaf-to-air temperature relationships have important consequences for modelling ecosystem fluxes, as leaf temperatures are often decoupled from local air temperature (Michaletz *et al.*, 2015, 2016). While our corrected results agree with prior results showing that limited homeothermy is common (Gates *et al.*, 1964; Linacre, 1964; Paw U, 1984; Upchurch & Mahan, 1988; Dong *et al.*, 2017; Blonder *et al.*, 2020; Yi *et al.*, 2020; Cook *et al.*, 2021), under other measurement conditions limited homeothermy may not be observed (Blonder & Michaletz, 2018; Drake *et al.*, 2020; Cook *et al.*, 2021; Miller *et al.*, 2021). As we show here, the LI-6400XT is a poor instrument for accurately observing leaf thermoregulatory behaviour. Alternative promising approaches for estimating leaf temperatures *in situ* include using the LI-6800, infrared thermography that also characterises the shaded leaf area (Jones, 2004; C. Still *et al.*, 2019; Blonder *et al.*, 2020), and stable oxygen isotopes (Helliker & Richter, 2008; Drake *et al.*, 2020).

Effects of temperature error on A–T response

Correcting an A–T curve for leaf temperature errors resulted in a narrowed curve, with a significant increase in T_{opt} and decrease in $T_{breadth}$. We found a substantial increase in E_a, although this did not rise to the level of significance, probably due to the small sample size and difficulty of estimating E_a with a high degree of confidence. A–T data obtained with the LI-6400XT may therefore underestimate the temperature sensitivity of photosynthesis. This has impacts across the field, since A–T curves are used to predict the effects of warming on plant function (Slot & Winter, 2017; Mau *et al.*, 2018), assess acclimation to persistent temperature changes (Sage & Kubien, 2007; Way & Yamori, 2014; Yamori *et al.*, 2014), and improve ESMs (Rogers *et al.*, 2017). $T_{breadth}$ and E_a are used to quantify the temperature sensitivity of photosynthesis, leaf thermal strategies, and macroecological metabolic temperature dependence (Michaletz *et al.*, 2015, 2016; Michaletz, 2018). $T_{breadth}$ is a key measurement of species' thermal niche, influencing productivity, physiological tolerance to extreme temperatures and climatic variability, and geographical distribution (Janzen, 1967; Stevens, 1989; Tewksbury *et al.*, 2008; Araújo *et al.*, 2013; Sunday *et al.*, 2014; Vasseur *et al.*, 2014; Perez *et al.*, 2016). Errors affecting these parameters may substantially impede our ability to accurately forecast the effects of climate change on plant demography, biogeography and productivity.

Effects of temperature error on A–C_i temperature response

Correcting A–C_i curves for leaf temperature errors resulted in discrepancies in estimates of V_{cmax}, J_{max} and their temperature dependencies. These parameters are used in ESMs to describe carbon uptake by vegetation (Rogers *et al.*, 2017). Variation in these parameters strongly affects predicted carbon uptake (Stinziano *et al.*, 2019), with substantial implications for climate change predictions. We found that 50% of the primary data sources retrieved from a large A–C_i compilation (Kumarathunge *et al.*, 2019) used a LI-6400/LI-6400XT with Peltier devices to force $T_{block,LI}$ away from T_{amb}. Therefore, we estimate that roughly half of the V_{cmax} and J_{max} kinetics data used in ESMs is subject to the errors described here. ESMs are particularly sensitive to the parameterisation of V_{cmax} (Rogers, 2014; Jefferson *et al.*, 2017; Rogers *et al.*, 2017; Stinziano *et al.*, 2020), so reductions in V_{cmax} at high temperatures mean that current projections are likely to overestimate primary productivity in response to anticipated climate change.

Conclusion

We demonstrated large biases in gas exchange measurements obtained with the LI-6400XT when internal machine temperatures depart from ambient. The nature of these biases is likely to be specific to individual machines and environmental conditions, requiring corrections to be particular to each set of measurement conditions. Our results contribute to a growing literature suggesting substantial challenges with gas exchange measurements, including errors in leaf and air temperatures (Mott & Peak, 2011; C. J. Still *et al.*, 2019). Other studies have found errors caused by leaky cuvette gaskets, respiration of leaf tissue enclosed under gaskets, and lateral gas diffusion within leaf intercellular airspaces (Long & Bernacchi, 2003; Jahnke & Pieruschka, 2006). Recent studies have also pointed out deficiencies in the theory used to compute quantities of interest, including subsaturating water vapour pressure within leaf airspaces (Cernusak *et al.*, 2018), nondiffusive water transport processes (Aparecido *et al.*, 2020), and inadequate accounting for cuticular conductance (Márquez *et al.*, 2021), which may equal stomatal conductance at high leaf temperatures (Duursma *et al.*, 2019; Slot *et al.*, 2021). These prior studies, and our results, underscore the difficulty of obtaining high-quality gas exchange measurements.

The errors revealed here substantially affect variables including $T_{leaf,LI}$, $T_{air,LI}$, g_{sw}, g_{tw}, g_{tc}, C_i, V_{cmax}, J_{max} and T_{opt}. Future research must focus on revising estimates of these critical parameters using robust methods not subject to the errors described here. Our best predictions about climate change and its impacts on vegetation depend crucially on data obtained with gas exchange equipment, and therefore the need for validation and revision of these quantities is urgent. We hope our results provide a foundation for improved fidelity of gas exchange measurements using these indispensable machines.

Acknowledgements

The authors are grateful to the Li-Cor engineers and technical support staff who have over the years helped us to better understand how gas exchange analysers work. We also thank two anonymous reviewers for constructive comments on an earlier manuscript, and Richard Telford, Barbara Neto-Bradley, and other participants of the international Plant Functional Traits

Courses for sharing the code used to load and manipulate raw Li-Cor data files in R. Finally, we thank Amy Angert, Rob Guy and Matt Pennell for the use of their Li-Cor instruments. This research was supported by Natural Sciences and Engineering Research Council of Canada (NSERC) Discovery and New Frontiers in Research Fund-Exploration (NFRF-2018-02043) grants to STM, an NSERC PGS-D grant to HAB, and an NSERC CGS-M to JCG.

Author contributions

JCG, HAB, IB and STM designed the research. JCG, HAB and IB collected new data. JCG, BB, JRS and STM contributed data for error propagation and correction analyses. JCG analysed the data with guidance from JRS and STM. JCG wrote the first draft of the manuscript, and JCG, HAB, BB, JRS and STM revised the manuscript.

ORCID

Benjamin Blonder https://orcid.org/0000-0002-5061-2385
Isaac Borrego https://orcid.org/0000-0003-1007-8963
Haley A. Branch https://orcid.org/0000-0003-0886-1836
Josef C. Garen https://orcid.org/0000-0002-3338-6662
Sean T. Michaletz https://orcid.org/0000-0003-2158-6525
Joseph R. Stinziano https://orcid.org/0000-0002-7628-4201

Data availability

Full data and code used for the production of figures and statistics in this article are available at https://github.com/MichaletzLab/LI-COR-thermal-gradients. Post-measurement correction functions and example analysis are also provided at the same location.

References

Allen AP, Gillooly JF, Brown JH. 2005. Linking the global carbon cycle to individual metabolism. *Functional Ecology* **19**: 202–213.

Angilletta MJ. 2006. Estimating and comparing thermal performance curves. *Journal of Thermal Biology* **31**: 541–545.

Aparecido LMT, Woo S, Suazo C, Hultine KR, Blonder B. 2020. High water use in desert plants exposed to extreme heat. *Ecology Letters* **23**: 1189–1200.

Araújo MB, Ferri-Yáñez F, Bozinovic F, Marquet PA, Valladares F, Chown SL. 2013. Heat freezes niche evolution. *Ecology Letters* **16**: 1206–1219.

Auguie B. 2017. *gridExtra: miscellaneous functions for 'Grid' graphics*. R package v.2.3. [WWW document] URL https://CRAN.R-project.org/package=gridExtra [accessed 12 April 2021].

Ball JT, Woodrow IE, Berry JA. 1987. A model predicting stomatal conductance and its contribution to the control of photosynthesis under different environmental conditions. In: Biggins J, ed. *Progress in photosynthesis research, vol. IV*. Dordrecht, the Netherlands: Springer, 221–224.

Bergman T, Lavine A, Incropera FP, DeWitt DP. 2011. *Fundamentals of heat and mass transfer, 7th edn*. Hoboken, NJ, USA: John Wiley & Sons.

Blonder B, Escobar S, Kapás RE, Michaletz ST. 2020. Low predictability of energy balance traits and leaf temperature metrics in desert, montane, and alpine plant communities. *Functional Ecology* **34**: 1882–1897.

Blonder B, Michaletz ST. 2018. A model for leaf temperature decoupling from air temperature. *Agricultural and Forest Meteorology* **262**: 354–360.

Brown JH, Gillooly JF, Allen AP, Savage VM, West GB. 2004. Toward a metabolic theory of ecology. *Ecology* **85**: 1771–1789.

Cernusak LA, Ubierna N, Jenkins MW, Garrity SR, Rahn T, Powers HH, Hanson DT, Sevanto S, Wong SC, McDowell NG *et al.* 2018. Unsaturation of vapour pressure inside leaves of two conifer species. *Scientific Reports* **8**: 7667.

Cook AM, Berry N, Milner KV, Leigh A. 2021. Water availability influences thermal safety margins for leaves. *Functional Ecology* **35**: 2179–2189.

Cramer W, Bondeau A, Woodward FI, Prentice IC, Betts RA, Brovkin V, Cox PM, Fisher V, Foley JA, Friend AD *et al.* 2001. Global response of terrestrial ecosystem structure and function to CO_2 and climate change: results from six dynamic global vegetation models. *Global Change Biology* **7**: 357–373.

Dong N, Prentice IC, Harrison SP, Song QH, Zhang YP. 2017. Biophysical homoeostasis of leaf temperature: a neglected process for vegetation and land-surface modelling. *Global Ecology and Biogeography* **26**: 998–1007.

Drake JE, Harwood R, Vårhammar A, Barbour MM, Reich PB, Barton CVM, Tjoelker MG. 2020. No evidence of homeostatic regulation of leaf temperature in *Eucalyptus parramattensis* trees: integration of CO_2 flux and oxygen isotope methodologies. *New Phytologist* **228**: 1511–1523.

Duursma RA. 2015. Plantecophys – an R package for analysing and modelling leaf gas exchange data. *PLoS ONE* **10**: e0143346.

Duursma RA, Blackman CJ, Lopéz R, Martin-StPaul NK, Cochard H, Medlyn BE. 2019. On the minimum leaf conductance: its role in models of plant water use, and ecological and environmental controls. *New Phytologist* **221**: 693–705.

Eyring V, Bony S, Meehl GA, Senior CA, Stevens B, Stouffer RJ, Taylor KE. 2016. Overview of the coupled model intercomparison project phase 6 (CMIP6) experimental design and organization. *Geoscientific Model Development* **9**: 1937–1958.

Farquhar GD, von Caemmerer S, Berry JA. 1980. A biochemical model of photosynthetic CO_2 assimilation in leaves of C_3 species. *Planta* **149**: 78–90.

Franks PJ, Bonan GB, Berry JA, Lombardozzi DL, Holbrook NM, Herold N, Oleson KW. 2018. Comparing optimal and empirical stomatal conductance models for application in Earth system models. *Global Change Biology* **24**: 5708–5723.

Galmés J, Hermida-Carrera C, Laanisto L, Niinemets Ü. 2016. A compendium of temperature responses of Rubisco kinetic traits: variability among and within photosynthetic groups and impacts on photosynthesis modeling. *Journal of Experimental Botany* **67**: 5067–5091.

Gates DM. 1980. *Biophysical Ecology*. New York, NY, USA: Springer-Verlag.

Gates DM, Hiesey WM, Milner HW, Nobs MA. 1964. Temperatures of *Mimulus* leaves in natural environments and in a controlled chamber. *Carnegie Institute Washington Yearbook* **63**: 418–428.

Hanson DT, Sharkey TD. 2001. Effect of growth conditions on isoprene emission and other thermotolerance-enhancing compounds. *Plant, Cell & Environment* **24**: 929–936.

Helliker BR, Richter SL. 2008. Subtropical to boreal convergence of tree-leaf temperatures. *Nature* **454**: 511–514.

Intergovernmental Panel on Climate Change (IPCC). 2021. Climate change 2021: the physical science basis. In: Masson-Delmotte VP *et al.*, eds. *Working group I contribution to the sixth assessment report of the intergovernmental panel on climate change*. Cambridge, UK: Cambridge University Press.

Jahnke S, Pieruschka R. 2006. Air pressure in clamp-on leaf chambers: a neglected issue in gas exchange measurements. *Journal of Experimental Botany* **57**: 2553–2561.

Janzen DH. 1967. Why mountain passes are higher in the tropics. *The American Naturalist* **101**: 233–249.

Jefferson JL, Maxwell RM, Constantine PG. 2017. Exploring the sensitivity of photosynthesis and stomatal resistance parameters in a land surface model. *Journal of Hydrometeorology* **18**: 897–915.

Jones HG. 2004. Application of thermal imaging and infrared sensing in plant physiology and ecophysiology. *Advances in Botanical Research* **41**: 107–163.

Kattge J, Knorr W. 2007. Temperature acclimation in a biochemical model of photosynthesis: a reanalysis of data from 36 species. *Plant, Cell & Environment* **30**: 1176–1190.

Kontopoulos D-G, García-Carreras B, Sal S, Smith TP, Pawar S. 2018. Use and misuse of temperature normalisation in meta-analyses of thermal responses of biological traits. *PeerJ* **6**: e4363.

Krinner G, Viovy N, de Noblet-Ducoudré N, Ogée J, Polcher J, Friedlingstein P, Ciais P, Sitch S, Prentice IC. 2005. A dynamic global vegetation model for studies of the coupled atmosphere-biosphere system. *Global Biogeochemical Cycles* **19**: GB1015.

Kumarathunge DP, Medlyn BE, Drake JE, Tjoelker MG, Aspinwall MJ, Battaglia M, Cano FJ, Carter KR, Cavaleri MA, Cernusak LA *et al.* 2019. Acclimation and adaptation components of the temperature dependence of plant photosynthesis at the global scale. *New Phytologist* **222**: 768–784.

Leuning R. 1995. A critical appraisal of a combined stomatal-photosynthesis model for C3 plants. *Plant, Cell & Environment* **18**: 339–355.

Li-Cor Biosciences Inc. 2012. *Using the LI-6400/LI-6400XT portable photosynthesis system.* Lincoln, NE, USA: Li-Cor Biosciences Inc.

Li-Cor Biosciences Inc. 2019. *Using the LI-6800 portable photosynthesis system.* Lincoln, NE, USA: Li-Cor Biosciences Inc.

Linacre ET. 1964. A note on a feature of leaf and air temperatures. *Agricultural Meteorology* **1**: 66–72.

Long SP, Bernacchi CJ. 2003. Gas exchange measurements, what can they tell us about the underlying limitations to photosynthesis? Procedures and sources of error. *Journal of Experimental Botany* **54**: 2393–2401.

Márquez DA, Stuart-Williams H, Farquhar GD. 2021. An improved theory for calculating leaf gas exchange more precisely accounting for small fluxes. *Nature Plants* **7**: 317–326.

Mau AC, Reed SC, Wood TE, Cavaleri MA. 2018. Temperate and tropical forest canopies are already functioning beyond their thermal thresholds for photosynthesis. *Forests* **9**: 47.

Medlyn BE, Dreyer E, Ellsworth D, Forstreuter M, Harley PC, Kirschbaum MUF, Roux XL, Montpied P, Strassemeyer J, Walcroft A *et al.* 2002. Temperature response of parameters of a biochemically based model of photosynthesis. II. A review of experimental data. *Plant, Cell & Environment* **25**: 1167–1179.

Medlyn BE, Duursma RA, Eamus D, Ellsworth DS, Prentice IC, Barton CVM, Crous KY, Angelis PD, Freeman M, Wingate L. 2011. Reconciling the optimal and empirical approaches to modelling stomatal conductance. *Global Change Biology* **17**: 2134–2144.

Michaletz ST. 2018. Evaluating the kinetic basis of plant growth from organs to ecosystems. *New Phytologist* **219**: 37–44.

Michaletz ST, Weiser MD, McDowell NG, Zhou J, Kaspari M, Helliker BR, Enquist BJ. 2016. The energetic and carbon economic origins of leaf thermoregulation. *Nature Plants* **2**: 16129.

Michaletz ST, Weiser MD, Zhou J, Kaspari M, Helliker BR, Enquist BJ. 2015. Plant thermoregulation: energetics, trait–environment interactions, and carbon economics. *Trends in Ecology & Evolution* **30**: 714–724.

Miller BD, Carter KR, Reed SC, Wood TE, Cavaleri MA. 2021. Only sun-lit leaves of the uppermost canopy exceed both air temperature and photosynthetic thermal optima in a wet tropical forest. *Agricultural and Forest Meteorology* **301–302**: 108347.

Miner GL, Bauerle WL. 2017. Seasonal variability of the parameters of the Ball–Berry model of stomatal conductance in maize (*Zea mays* L.) and sunflower (*Helianthus annuus* L.) under well-watered and water-stressed conditions. *Plant, Cell & Environment* **40**: 1874–1886.

Monteith JL, Unsworth MH, eds. 2013. *Principles of environmental physics.* Boston, MA, USA: Academic Press.

Mott KA, Peak D. 2011. Alternative perspective on the control of transpiration by radiation. *Proceedings of the National Academy of Sciences, USA* **108**: 19820–19823.

Padfield D, O'Sullivan H, Pawar S. 2021. *rTPC* and *nls.multstart*: a new pipeline to fit thermal performance curves in R. *Methods in Ecology and Evolution* **12**: 1138–1143.

Paw U KT. 1984. A theoretical basis for the leaf equivalence point temperature. *Agricultural Meteorology* **30**: 247–256.

Perez TM, Stroud JT, Feeley KJ. 2016. Thermal trouble in the tropics. *Science* **351**: 1392–1393.

R Core Team. 2019. *R: a language and environment for statistical computing.* v.3.6.2. Vienna, Austria: R Foundation for Statistical Computing.

Reich PB, Tjoelker MG, Machado J-L, Oleksyn J. 2006. Universal scaling of respiratory metabolism, size and nitrogen in plants. *Nature* **439**: 457–461.

Rogers A. 2014. The use and misuse of $V_{c,max}$ in earth system models. *Photosynthesis Research* **119**: 15–29.

Rogers A, Medlyn BE, Dukes JS, Bonan G, von Caemmerer S, Dietze MC, Kattge J, Leakey ADB, Mercado LM, Niinemets Ü *et al.* 2017. A roadmap for improving the representation of photosynthesis in Earth system models. *New Phytologist* **213**: 22–42.

Sage RF, Kubien DS. 2007. The temperature response of C_3 and C_4 photosynthesis. *Plant, Cell & Environment* **30**: 1086–1106.

Schoolfield RM, Sharpe PJH, Magnuson CE. 1981. Non-linear regression of biological temperature-dependent rate models based on absolute reaction-rate theory. *Journal of Theoretical Biology* **88**: 719–731.

Slot M, Garcia MN, Winter K. 2016. Temperature response of CO_2 exchange in three tropical tree species. *Functional Plant Biology* **43**: 468–478.

Slot M, Nardwattanawong T, Hernández GG, Bueno A, Riederer M, Winter K. 2021. Large differences in leaf cuticle conductance and its temperature response among 24 tropical tree species from across a rainfall gradient. *New Phytologist* **232**: 1618–1631.

Slot M, Winter K. 2017. *In situ* temperature response of photosynthesis of 42 tree and liana species in the canopy of two Panamanian lowland tropical forests with contrasting rainfall regimes. *New Phytologist* **214**: 1103–1117.

Stevens GC. 1989. The latitudinal gradient in geographical range: how so many species coexist in the tropics. *The American Naturalist* **133**: 240–256.

Still C, Powell R, Aubrecht D, Kim Y, Helliker B, Roberts D, Richardson AD, Goulden M. 2019. Thermal imaging in plant and ecosystem ecology: applications and challenges. *Ecosphere* **10**: e02768.

Still CJ, Sibley A, Page G, Meinzer FC, Sevanto S. 2019. When a cuvette is not a canopy: a caution about measuring leaf temperature during gas exchange measurements. *Agricultural and Forest Meteorology* **279**: 107737.

Stinziano J, Harjoe M, Roback C, Toliver N, Rogers A, Hanson DT. 2020. Photosynthetic capacity exhibits diurnal variation, implications for terrestrial biosphere models and gas exchange measurements. *Authorea.* doi: 10.22541/au.160133681.10036922.

Stinziano JR, Bauerle WL, Way DA. 2019. Modelled net carbon gain responses to climate change in boreal trees: Impacts of photosynthetic parameter selection and acclimation. *Global Change Biology* **25**: 1445–1465.

Sunday JM, Bates AE, Kearney MR, Colwell RK, Dulvy NK, Longino JT, Huey RB. 2014. Thermal-safety margins and the necessity of thermoregulatory behavior across latitude and elevation. *Proceedings of the National Academy of Sciences, USA* **111**: 5610–5615.

Tewksbury JJ, Huey RB, Deutsch CA. 2008. ECOLOGY: putting the heat on tropical animals. *Science* **320**: 1296–1297.

Upchurch DR, Mahan JR. 1988. Maintenance of constant leaf temperature by plants—II. Experimental observations in cotton. *Environmental and Experimental Botany* **28**: 359–366.

Vasseur DA, DeLong JP, Gilbert B, Greig HS, Harley CDG, McCann KS, Savage V, Tunney TD, O'Connor MI. 2014. Increased temperature variation poses a greater risk to species than climate warming. *Proceedings of the Royal Society B: Biological Sciences* **281**: 20132612.

Venturas MD, Mackinnon ED, Jacobsen AL, Pratt RB. 2015. Excising stem samples underwater at native tension does not induce xylem cavitation: no evidence for a tension-cutting artefact. *Plant, Cell & Environment* **38**: 1060–1068.

Way DA, Yamori W. 2014. Thermal acclimation of photosynthesis: on the importance of adjusting our definitions and accounting for thermal acclimation of respiration. *Photosynthesis Research* **119**: 89–100.

Wickham H. 2009. *ggplot2: elegant graphics for data analysis.* New York, NY, USA: Springer-Verlag.

Wickham H, Averick M, Bryan J, Chang W, McGowan LD, François R, Grolemund G, Hayes A, Henry L, Hester J *et al.* 2019. Welcome to the tidyverse. *Journal of Open Source Software* **4**: 1686.

Wright IJ, Reich PB, Westoby M, Ackerly DD, Baruch Z, Bongers F, Cavender-Bares J, Chapin T, Cornelissen JHC, Diemer M *et al.* 2004. The worldwide leaf economics spectrum. *Nature* **428**: 821–827.

Wu J, Serbin SP, Ely KS, Wolfe BT, Dickman LT, Grossiord C, Michaletz ST, Collins AD, Detto M, McDowell NG *et al.* 2020. The response of stomatal conductance to seasonal drought in tropical forests. *Global Change Biology* **26**: 823–839.

Yamori W, Hikosaka K, Way DA. 2014. Temperature response of photosynthesis in C_3, C_4, and CAM plants: temperature acclimation and temperature adaptation. *Photosynthesis Research* **119**: 101–117.

Yi K, Smith JW, Jablonski AD, Tatham EA, Scanlon TM, Lerdau MT, Novick KA, Yang X. 2020. High heterogeneity in canopy temperature among co-occurring tree species in a temperate forest. *Journal of Geophysical Research Biogeosciences* **125**: e2020JG005892.

Supporting Information

Additional Supporting Information may be found online in the Supporting Information section at the end of the article.

Fig. S1 Relationships between leaf temperatures measured by thermocouples threaded into leaf secondary veins ($T_{leaf,thread}$) and thermocouples taped to abaxial leaf surfaces ($T_{leaf,lower}$).

Fig. S2 Agreement between thermocouples used in the experiments.

Fig. S3 Relationship between calculated and measured leaf temperatures.

Please note: Wiley Blackwell are not responsible for the content or functionality of any Supporting Information supplied by the authors. Any queries (other than missing material) should be directed to the *New Phytologist* Central Office.